Synchronization of electrochemical oscillators with differential coupling

Mahesh Wickramasinghe and István Z. Kiss*
Department of Chemistry, Saint Louis University, 3501 Laclede Avenue, St. Louis, Missouri 63103, USA
(Received 8 August 2013; published 10 December 2013)

Experiments are presented to describe the effect of capacitive coupling of two electrochemical oscillators during Ni dissolution in sulfuric acid solution. Equivalent circuit analysis shows that the coupling between the oscillators occurs through the difference between the differentials of the electrode potentials. The differential nature of the coupling introduces strong negative nonisochronicity (i.e., phase shear, strong dependence of the period on the amplitude) in the coupling mechanism with smooth oscillators (under conditions just above a Hopf bifurcation point). Because of the negative nonisochronicity, asymmetrically coupled oscillators exhibit anomalous phase synchronization in the form of frequency difference enhancement. At strong coupling bistability is observed between in-phase and antiphase synchronized states. With relaxation oscillators, in contrast to the resistive coupling where antiphase synchronization can occur, the typical system response with weak coupling is out-of-phase synchronization. When the capacitance is applied on the individual resistors attached to the electrodes the oscillators exhibit weak positive nonisochronicity; this is in contrast with the strong negative nonisochronicity obtained with cross coupling. The proposed coupling configurations reveal the importance of the nonisochronicity level of oscillations for the experimentally observed synchronization patterns and also provide efficient ways of tuning the nonisochronicity level of the oscillations. This latter feature can be exploited to design synchronization features with a combination of resistive (difference) and capacitive (differential) coupling.

DOI: 10.1103/PhysRevE.88.062911 PACS number(s): 05.45.Xt, 82.40.Bj, 82.40.Np

I. INTRODUCTION

Oscillatory chemical reactions carried out in discrete units often form synchronization patterns that have been studied with coupled continuous, stirred-tank reactors with homogeneous chemical reactions [1–6], surface reactions on heterogeneous catalyst particles [7–9], Belousov-Zhabotinsky beads [10–12] and droplets [13,14], and electrode arrays [15–18]. Even weak interactions between the units can induce patterns that strongly depend on the type of complex chemical reaction and the coupling mechanism and symmetry. In studies with electrochemical oscillators the coupling is often through potential drop in the electrolyte [19,20] or in externally attached coupling resistors [16,21]. In these examples, because the coupling is predominantly electrical, the physical form of the coupling depends on the difference between the electrode potentials of the electrodes [22]. Although the primary description often includes a qualitative characterization of the synchronization pattern (e.g., in-, anti-, or out-of-phase oscillations), quantitative description of the patterns requires a theoretical framework that considers fundamental oscillatory properties and the mathematical form of the coupling. For example, in weak-coupling approximations, a phase model description [23] is possible with the oscillator frequency, wave form, and phase sensitivity function (phase response curve).

The isochronicity level of the oscillator is an important property of the phase interaction function; the strong dependence of the oscillatory period on the amplitude results in high-level "shear" in the phase dynamics and coupling can dramatically change the oscillatory period [23–25]. The classical Kuramoto model with a $\sin(\Delta\varphi)$ interaction function considers isochronous oscillators; nonisochronicity can be taken into account with a shift α in the interaction function [$\sin(\Delta\varphi+\alpha)$]. Strongly nonisochronous oscillators often form rich synchronization patterns [26–29]. For example, in pairs of asymmetrically coupled oscillators "anomalous" phase synchronization effects were reported in the form of advanced or delayed synchronization and frequency difference enhancement or inversion [25,27,30,31]; in globally coupled oscillators diffusion-induced inhomogeneity can occur in the form of periodic or quasiperiodic amplitude clusters [28]. In a previous work [32], by increasing the temperature of oscillatory Ni dissolution from 10 to 20 °C, nonisochronicity of asymmetrically coupled oscillators resulted in advanced or delayed synchronization depending on the relative frequencies of the driver and follower oscillators.

Although most electrochemical synchronization studies have been performed with electrical "difference" coupling [21], other types of coupling between electrodes are possible. For example, in the pioneering work of Franck and Meunier in 1953, several synchronization patterns were reported with capacitive coupling of electrochemical oscillators [33]. Coupling through the charging current could strongly affect the dynamics of electrode arrays, especially with large electrode sizes and large capacitive current contributions or with adsorption of charged species that are also often modeled by capacitive terms [34]. The coupling through capacitors occurs through the time derivatives of the potentials. Therefore, coupling through capacitances could induce a synchronization structure; this is different from the previously studied resistive (difference) coupling.

In this paper, we investigate coupling induced by a capacitance in dual-electrode experiments with oscillatory nickel electrodissolution [35]. Equivalent circuit analysis is applied to explore the nature of the coupling. The isochronicity level of the interactions is analyzed with frequency vs coupling strength diagrams and experiment-based phase models [36]

*Corresponding author: izkiss@slu.edu

with smooth oscillations that occur through a Hopf bifurcation. A test for the capability of capacitive coupling to produce anomalous phase synchronization is performed with coupling of electrodes of different electrode sizes. With relaxation oscillators, the synchronization patterns are compared to those obtained with resistance coupling [16]. Finally, a short analysis is made to explore the scenario when the capacitance is applied on individual resistors attached to the electrode.

II. EXPERIMENTS

A. Experimental setup

A standard electrochemical cell consisting of two nickel working electrodes (Goodfellow Cambridge Ltd., 99.98%), a Hg-Hg_2SO_4–saturated K_2SO_4 reference electrode, and a platinum counterelectrode in 3 mol/l sulfuric acid was used in the experiments [see Fig. 1(a)]. The two working electrodes have identical diameters for symmetrical or different diameters for asymmetrical coupling [32]. The wires were embedded in epoxy with at least 5 mm spacing between them. The reactions take place only at the ends of the exposed area, which is wet polished on a series of sandpapers (P180–P4000) with a Buehler Metaserv 3000 polisher. The experiments were carried out with (1 mm, 1 mm) and (1 mm, 2 mm) working electrode diameter combinations at 10 °C maintained by a Neslab RTE-7 circulating bath. External individual resistances $R_{\mathrm{ind},1}$ and $R_{\mathrm{ind},2}$ [see Fig. 1(a)] were added to each electrode. Typical values of individual resistances were 1000 Ω and 225 Ω for 1-mm- and 2-mm-diameter electrodes, respectively, such that $R_{\mathrm{ind}}A = 8{-}9\ \Omega\,\mathrm{cm}^2$ for each electrode. The currents of the electrodes were digitized with a National Instruments PCI 6255 data acquisition board with 200–1000 Hz data acquisition rate. The electrode array connected to a potentiostat (ACM Instruments, Gill AC) was polarized at a constant circuit potential V. (All potentials are given with respect to the reference electrode.) The electrodes were coupled with a combination of resistance (R varied between 3 and 1000 kΩ) and capacitance (C = 1–1000 μF) parallel to each other. (In some experiments only resistance or capacitance was used.)

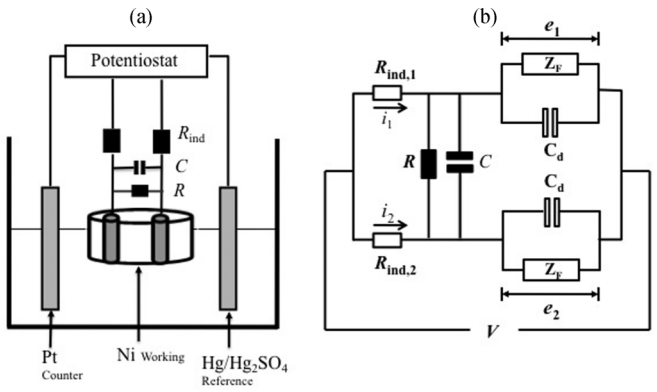

FIG. 1. Schematic and equivalent circuit of experimental setup. (a) Schematic diagram of standard three-electrode electrochemical cell. R_{ind}, Individual resistance; R, coupling resistance; C, coupling capacitance. (b) The equivalent circuit. V, Circuit potential; e_1,e_2, electrode potentials; Z_F, Faraday impedance; C_d, double-layer capacitance; i_1, i_2, currents.

A typical data file consists of about 105 (uncoupled) or 280 (close to synchronization) oscillations with about 1750 data points per cycle.

B. Frequency of oscillations

For smooth oscillators, the Hilbert transform [37] of the time series of the current,

$$H(t) = \frac{1}{\pi}\mathrm{P}\int_{-\infty}^{\infty}\frac{i(\tau)-\langle i\rangle}{t-\tau}d\tau, \tag{1}$$

is used in defining the phase using the derivative Hilbert transform approach [38]:

$$\phi(t) = \tan^{-1}\frac{dH[i(t)]/dt}{di(t)/dt}. \tag{2}$$

P in Eq. (1) implies that the integral should be evaluated in the sense of the Cauchy principal value. $\langle i\rangle$ is the temporal average of the time series $i(t)$. The frequency ω of an oscillator is obtained from a linear fit of the unwrapped $\phi(t)$ vs t:

$$\omega = \frac{1}{2\pi}\left\langle\frac{d\phi}{dt}\right\rangle. \tag{3}$$

C. Reduced frequency and coupling strength

The natural frequency of an oscillator (uncoupled oscillators) in our system drifts by about ±20 mHz in a single direction in a time frame of about 3 h. A reduced frequency and reduced frequency difference are introduced in order to mitigate the effects of the drift [32]. The natural frequencies of the two oscillators are calculated from consecutive time series collected before coupling and after a coupling experiment. Four uncoupled frequency values define the mean natural frequency ω_0. The mean value of the natural frequency difference ($\Delta\omega = \omega_2 - \omega_1$) between the oscillators before and after the coupling experiments is denoted as $\Delta\omega_0$. The natural frequency difference $\Delta\omega_0$ was maintained at 5–30 mHz throughout the experiments. If the frequency difference fell out of this range small adjustments (maximum ± 10%) of the individual resistors were made to reset the natural frequency difference. To calculate the reduced frequency, the frequency $\omega_{1,2}$ of an oscillator at a certain coupling strength is rescaled as $(\omega_{1,2} - \omega_0)/\Delta\omega_0$. Therefore, without coupling, oscillators 1 (slow) and 2 (fast) always have rescaled frequencies of −0.5 and 0.5, respectively. (Note that because of the natural drift of the oscillators this rescaling was performed even for the uncoupled oscillators.) Similarly, the frequency difference between the oscillators ($\Delta\omega = \omega_2 - \omega_1$) is rescaled as $(\omega_2 - \omega_1)/\Delta\omega_0$.

The coupling strength K between two oscillators coupled with resistance R is defined [32] as

$$K = \frac{1}{2}\left(\frac{1}{RA_1} + \frac{1}{RA_2}\right) = \frac{1}{2R\tilde{A}}, \tag{4}$$

where A_i are the areas of the electrodes and $\tilde{A}$ is the reduced area given by $1/\tilde{A} = 1/A_1 + 1/A_2$. Because the natural frequency difference between the oscillators varied from experiment to experiment, K is expressed by a reduced

coupling strength (K_r) defined as

$$K_r = \frac{K}{\Delta\omega_0} = \frac{1}{2R\tilde{A}\Delta\omega_0} \tag{5}$$

with units of $\Omega^{-1}\,\mathrm{cm}^{-2}\,\mathrm{s}$.

A similar definition is introduced for two oscillators coupled with a capacitance C:

$$K_c = \frac{K}{\Delta\omega_0} = \frac{C}{2\tilde{A}\Delta\omega_0}. \tag{6}$$

D. Interaction function

The dynamics of the coupled oscillator system is analyzed in the framework of the phase description [23], [39]:

$$\frac{d\phi_1}{dt} = \Omega_{1,0} + \Gamma(\Delta\phi), \tag{7}$$

$$\frac{d\phi_2}{dt} = \Omega_{2,0} + \Gamma(-\Delta\phi), \tag{8}$$

where ϕ_i and $\Omega_{i,0}$ are the phase and natural frequency (in rad/s), respectively, of the ith oscillator, $\Delta\phi = \phi_2 - \phi_1$ is the phase difference, and Γ is the interaction function. The interaction function describes the effect of coupling on the instantaneous frequencies. Γ can be determined from an experiment close to the onset of phase synchronization when the phase difference displays phase slipping behavior [40]. For the kth oscillatory cycle, the peak-to-peak period can be calculated [$T(k)$], from which the instantaneous frequency of the oscillations at any time between the two corresponding peaks can be obtained as $\Omega(t) = 2\pi/T(k)$. The Γ function (for oscillator 1) can be obtained [40–43] by plotting the quantity $\Omega_1(t) - \Omega_{1,0}$ of the oscillator as a function of the phase difference $\Delta\phi$. Note that in these calculations the linear interpolation method [44] is used for calculating the phase, where at the kth oscillatory peak the phase is set to $k \times 2\pi$ and for other times linear interpolation is applied (a similar approach was used for definition of the phase for relaxation oscillators).

III. RESULTS AND DISCUSSION

A. Coupling with cross capacitance

First we consider the coupling induced by a resistance or capacitance inserted between the two electrodes as shown in Fig. 1(a).

1. Theory

To evaluate the coupling induced by parallel resistance or capacitance, we analyze the equivalent circuit of the two-electrode electrochemical system shown in Fig. 1(b). The currents of the electrodes (i_1 and i_2) pass through the individual resistors ($R_{\mathrm{ind},1}$ and $R_{\mathrm{ind},2}$) connected to electrodes that have capacitance per surface area C_d. The electrochemical system acts as a complex impedance element (Z_F) with given characteristics of a Faraday current density (j_F) as a function of the electrode potentials (e_1 and e_2). The coupling between the electrodes is imposed by the cross resistance (R) and capacitance (C). The circuit potential V is kept constant:

$$\begin{aligned} V &= e_1 + i_1 R_{\mathrm{ind},1}, \\ V &= e_2 + i_2 R_{\mathrm{ind},2}. \end{aligned} \tag{9}$$

The currents of the electrodes have three sources: the capacitive currents ($A_{1,2}C_d de_{1,2}/dt$), the Faraday currents [$A_{1,2}j_F(e_{1,2})$], and the coupling currents through the resistance [$(e_2 - e_1)/R$] and capacitance [$C(de_2/dt - de_1/dt)$]:

$$\begin{aligned} i_1 &= A_1 j_F(e_1) + A_1 C_d \frac{de_1}{dt} + \frac{e_2 - e_1}{R} + C\left(\frac{de_2}{dt} - \frac{de_1}{dt}\right), \\ i_2 &= A_2 j_F(e_2) + A_2 C_d \frac{de_2}{dt} + \frac{e_2 - e_1}{R} - C\left(\frac{de_2}{dt} - \frac{de_1}{dt}\right). \end{aligned} \tag{10}$$

By combining Eqs. (9) and (10) the equations for the dynamical evolution of the electrode potential can be obtained as

$$\begin{aligned} C_d \frac{de_1}{dt} &= \frac{V - e_1}{A_1 R_{\mathrm{ind},1}} - j_F(e_1) + \frac{e_2 - e_1}{A_1 R} \\ &\quad + \frac{C}{A_1}\left(\frac{de_2}{dt} - \frac{de_1}{dt}\right), \\ C_d \frac{de_2}{dt} &= \frac{V - e_2}{A_2 R_{\mathrm{ind},2}} - j_F(e_2) + \frac{e_1 - e_2}{A_2 R} \\ &\quad + \frac{C}{A_2}\left(\frac{de_1}{dt} - \frac{de_2}{dt}\right). \end{aligned} \tag{11}$$

These equations are identical to those obtained with resistive coupling [32] except for the last term which represents the coupling induced by the capacitance.

The coupling induced by the capacitance is fundamentally different from the coupling induced by the resistance; the latter depends on the difference between the electrode potentials while the former depends on the difference between the derivatives of the electrode potentials. For simple sinusoidal oscillatory wave forms the derivative of the signal is equal to the signal shifted by $\pi/2$; therefore, it is expected that the purely capacitive coupling has a similar effect to delayed coupling with a time delay of 0.25 times the oscillatory period. Similarly, in phase model approximations, it would be expected that the delay shifts [45] the interaction function Γ by $\pi/2$ as a result of capacitive coupling. However, for strongly nonlinear relaxation oscillations the effect of this delay term is not trivial, since the Fourier harmonics of the oscillatory period are affected differently. Equation (11) also shows that when the combined effect of resistive (difference) and capacitive (differential) coupling is studied, by keeping the RC charging time constant, the effect of coupling strength can be investigated without changing the type (relative ratio of the coupling terms) of the interactions.

2. Experiments with two smooth oscillators

To investigate the effect of the capacitive coupling on the dynamics of electrochemical oscillators, we perform experiments with oscillations close to a Hopf bifurcation (smooth oscillators) and oscillations close to a homoclinic bifurcation (relaxation oscillators) [36].

a. Bistable states of synchronization. Two uncoupled smooth oscillators (with natural frequencies 0.364 and

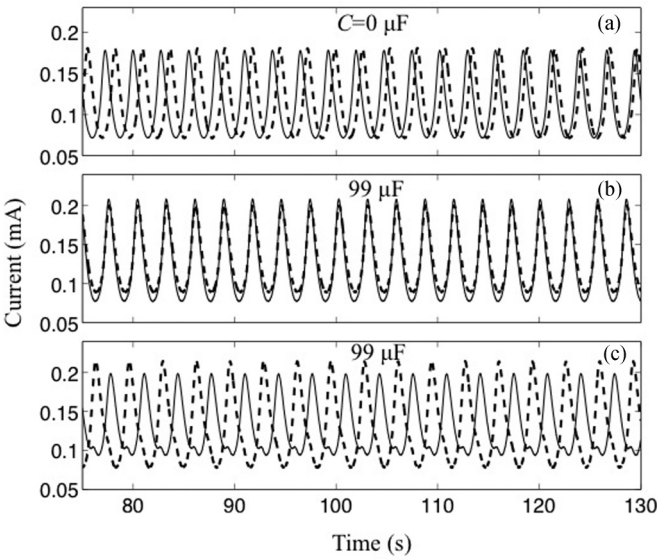

FIG. 2. Bistability between in- and antiphase synchronization of two smooth oscillators with pure capacitive coupling. (a) Current time series of two smooth oscillators without added coupling. (b) In-phase synchronization with coupling capacitance $C = 99\ \mu$F. (c) Antiphase synchronization with same coupling as in (b). $V = 1.085$ V; $R_{\rm ind} =$ 900–1000 Ω.

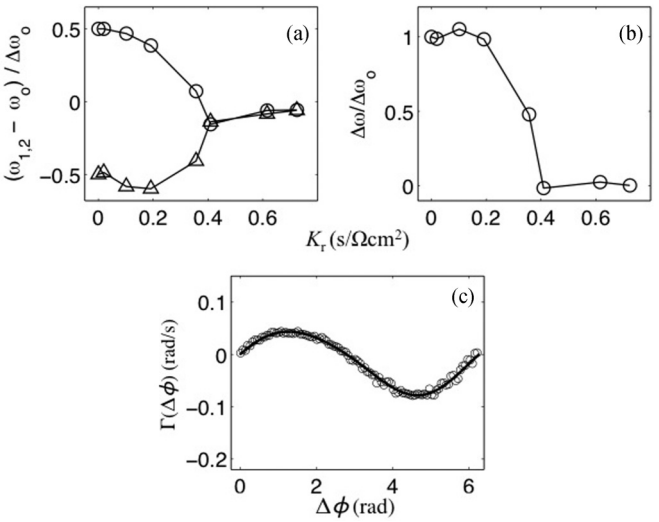

FIG. 3. Phase synchronization of two coupled smooth oscillators with resistive coupling. (a) Reduced frequency vs reduced coupling strength; $R = 50$–1000 kΩ. (b) Reduced frequency difference vs reduced coupling strength. (c) Interaction function vs phase difference measured at $K_r = 0.36$ s/Ω cm^2 ($R = 19$ kΩ). $V = 1.085$ V; $R_{\rm ind} =$ 1000–1030 Ω.

0.369 Hz) are shown in Fig. 2(a). The effects of pure capacitance coupling ($K_c = 1.5$ sF/cm^2) at coupling strengths above the synchronization transition are shown in Figs. 2(b) and 2(c). In experiments where the initial phase differences (at the moment of turning on the coupling) of the oscillators were relatively small, the oscillators exhibited in-phase synchronization with frequencies close to the average of the natural frequencies ($\omega_r = 0.0$) as shown in Fig. 2(b). However, when the initial phase differences between the oscillators were large, another mode of synchronization occurred in antiphase configuration [see Fig. 2(c)]; in this configuration the synchronization frequency ($\omega_r = -5.0$) is about 17% slower than the in-phase synchronized behavior. With resistive coupling the synchronized state in the given electrochemical system with smooth oscillators is in phase [16,36]; therefore, we see that capacitive coupling induces other types of synchronized state not seen with resistive coupling.

b. Capacitive-coupling-induced nonisochronicity. To further characterize the synchronization behavior, we determined the frequencies of the oscillators and the phase interaction function for coupling with resistance, capacitance, and combined resistance-capacitance. The transition to phase synchronization of two symmetrically coupled oscillators (1-mm-diameter electrodes) with resistive coupling is shown in Fig. 3. In the plot of reduced frequency vs reduced coupling strength [see Fig. 3(a)] we see that the oscillators become synchronized at $K_r^* = 0.41$ s/Ω cm^2. The slope of the reduced frequency with respect to the reduced coupling strength in the zero-coupling limit characterizes the extent of experimental nonisochronicity,

$$q_{1,2} = \lim_{K_r \to 0} \frac{d\left(\omega_{1,2} - \omega_0\right)/\Delta\omega_0}{dK_r} \qquad (12)$$

of oscillators [25] (this quantity is proportional to the amplitude of the cosine term of the phase interaction function). In resistively coupled systems, the oscillators exhibit small, different levels of nonisochronicities with $q_1 = -0.9\ \Omega\,\text{cm}^2\,\text{s}^{-1}$ and $q_2 = -0.3\ \Omega\,\text{cm}^2\,\text{s}^{-1}$, respectively. It is useful to calculate a dimensionless quantity to characterize the extent of nonisochronicity; because the critical coupling strength is proportional to the sinusoidal terms of the phase interaction function [25], the quantity qK_r^* is proportional to the ratio of the cosine and sine terms of the interaction function. For the experimental system $q_1 K_r^* = -0.37$ and $q_2 K_r^* = -0.12$.

The frequency difference vs coupling strength graph [Fig. 3(b)] shows that the frequency difference is in agreement with the classical formula [25] $\Delta\omega = \Delta\omega_0\sqrt{1 - K_r^2/K_r^{*2}}$. Small deviations (e.g., a small increase of the frequency difference) are due to the small, heterogeneous levels of nonisochronicities of the oscillators. The interaction function for resistively coupled systems is shown in Fig. 3(c); as was reported earlier [43] the interaction function contains mainly first-harmonic sinusoidal components and can be approximated with $\Gamma(\Delta\phi) = 0.020\pi\sin(\Delta\phi) - 0.004\pi\,[1 - \cos(\Delta\phi)]$. For two symmetrically coupled oscillators the cosine term of the interaction function is responsible for inducing nonisochronicity [23,24]. Thus we see that the measured interaction function properly predicts the weak nonisochronous character of the coupled system.

Phase synchronization with capacitive coupling is very different from that with resistive coupling. In the example shown in Fig. 4(a), the oscillators synchronized in antiphase configuration at around $K_c = 1$ sF/cm^2. This antiphase synchronization [corresponding to that shown in Fig. 2(c)] prevailed for $1 \leqslant K_c < 1.5$ sF/cm^2. For stronger coupling, $K_c \geqslant 1.5$ sF/cm^2, only the in-phase synchronized behavior was obtained. [The in-phase synchronized oscillations corresponding to those shown in Fig. 2(b) would have rescaled

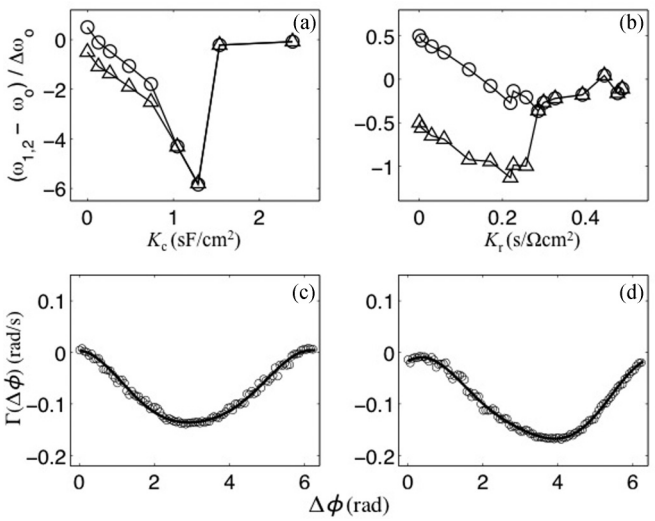

FIG. 4. Phase synchronization of two coupled smooth oscillators with capacitance (left column) and combined resistance-capacitance (right column) coupling causing negative nonisochronicity. Top row: Reduced frequency vs reduced coupling strength. Bottom row: Interaction function vs phase difference. Open circles, experimental data; solid line: fast Fourier transform fit using first harmonics. (a) C = 5–200 μF. (b) RC = 1s , R = 10–1000 kΩ. (c) $K_c = 0.24$ s F/cm^2 (C = 30 μF), V = 1.090 V. (d) $K_r = 0.46$ s/Ω cm^2, $K_c = 0.36$ s F/cm^2 (RC = 0.8 s). V = 1.085–1.120 V, $R_{\rm ind}$ = 900–1070 Ω.

frequency values of 0.] However, the major difference between the resistive and capacitive coupling is the presence of strong, negative nonisochronicities with $q_1 = -3.3$ cm^2 F^{-1} s^{-1} and $q_2 = -3.7$ cm^2 F^{-1} s^{-1}, in particular in comparison with the critical coupling strengths ($q_1 K_c^* = -3.3$, $q_2 K_c^* = -3.7$). With capacitive coupling, before the synchronization transition the frequencies of the oscillations decrease, and at the critical synchronization point the frequency is much lower than the natural frequency of the oscillators. The effect of strong nonisochronicity is also reflected in the interaction function determined at $K_c = 0.24$ s F/cm^2 (30 μF) as shown in Fig. 4(c). The interaction function $\Gamma(\Delta\phi) = -0.004\pi \sin(\Delta\phi) - 0.022\pi\,[1 - \cos(\Delta\phi)]$ shows weak sinusoidal and strong cosine components. Note that because of the presence of the strong cosine component, two symmetrically coupled oscillators would be expected to synchronize only at very high coupling strengths because the synchronized state is determined by the (positive) sinusoidal components of the interaction functions. At these very high coupling strengths there is often strong modulation of oscillation amplitudes, and thus the phase approximation may break down; the bistability between the in-phase and antiphase states shown in Figs. 2(b) and 2(c) can result from contributions of weak higher-harmonic positive sinusoidal components in the interaction functions (whose contributions are difficult to determine with good accuracy) or from amplitude effects.

The presence of a strong sinusoidal component with resistance and of a strong cosine component with capacitance coupling in the interaction function allows the tuning of the nonisochronicity level of the oscillatory system with proper RC values. Figure 4(b) shows the results obtained with RC = 0.8 s, where the time scale of the coupling element is comparable to the oscillation period (2.7 s). At these conditions the nonisochronicity levels ($q_1 = -4.7$ Ω cm^2 s^{-1} and $q_2 = -3.3$ Ω cm^2 s^{-1}) are between those observed for the resistive and capacitive coupling (e.g., $q_1 K_r^* = -1.1$, $q_2 K_r^* = -0.8$). In the synchronized state we observed only in-phase configuration, which is in agreement with the expected effect of a large first-harmonic sinusoidal term in the interaction function. The interaction function shown in Fig. 4(d) can be approximated with $\Gamma(\Delta\phi) = 0.012\pi \sin(\Delta\phi) - 0.022\pi\,[1 - \cos(\Delta\phi)]$ at K_r = 0.46 s/Ω cm^2 and K_c = 0.36 s F/cm^2 (RC = 0.8 s); note the more balanced contributions of sine and cosine components.

We have thus demonstrated that the capacitive coupling induces a negative nonisochronous character of the interactions between the oscillators. By combinations of resistance and capacitance coupling the relative ratio of the nonisochronicity can be controlled. Because the synchronization transition in many examples could depend on the level of nonisochronicity, it is expected that different synchronization patterns could be observed with capacitive coupling.

c. Anomalous phase synchronization with asymmetrical coupling. As a demonstration of a nontrivial synchronization effect due to the presence of nonisochronous interaction between the oscillators we performed experiments with asymmetrical coupling of oscillators with a combined resistance-capacitance coupling with RC = 1 s. The asymmetrical interaction is induced by coupling a 1-mm-diameter wire to a 2-mm-diameter wire. Because the coupling strength is inversely proportional to the surface areas of the electrodes [32] [e.g., see Eq. (11)] this configuration induces asymmetrical interactions. The coupling imposed by the 2-mm-diameter electrode on the 1-mm-diameter electrode is four times stronger than the coupling in the opposite direction. With increase of coupling the transition to phase synchronization is shown in Fig. 5(a). The natural frequency of the driver oscillator (2 mm) is 7% higher than that of the follower oscillator (1 mm). We observed that the frequency of the driver oscillator is affected only slightly by the coupling. The frequency of the follower electrode first decreases with increase of the coupling strength due to the presence of negative nonisochronicity (behavior strongly affected by the cosine term in Γ); when the coupling becomes strong phase synchronization takes place by a sudden increase of the frequency of the follower oscillator to match the frequency of the driver oscillator. Consequently, under these circumstances, the frequency difference variation as a function of the coupling strength exhibits a strong anomaly in comparison to the traditional route [shown in Fig. 3(b) with symmetrical coupling]; with increase of the coupling the frequency difference is enhanced from 1 (uncoupled) to 1.5 (at K_r = 0.15 s/Ω cm^2) before transition to synchronization takes place [see Fig. 5(b)].

Time series of the current density of the coupled oscillators are shown in Figs. 5(c) and 5(d) just before (K_r = 0.15 s/Ω cm^2) and after (K_r = 0.25 s/Ω cm^2) phase synchronization (PS) takes place, respectively. Strong amplitude modulation in the oscillations in the follower was observed before PS (as a result of relatively strong coupling and nonisochronicity). After PS took place a relatively large amplitude difference was observed between the oscillators; the amplitude of the follower oscillator diminished and remained nearly constant.

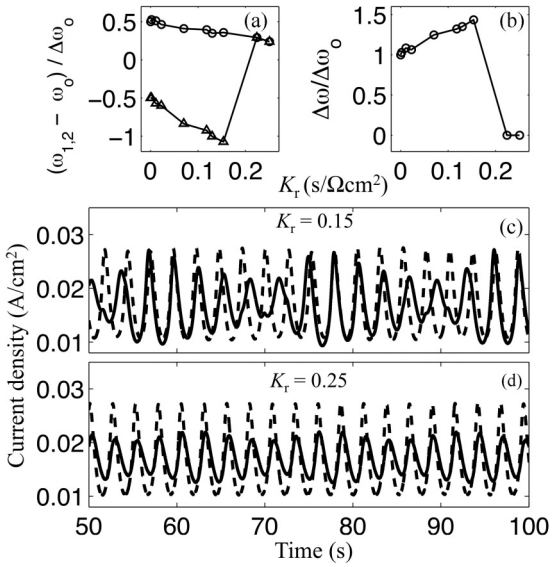

FIG. 5. Phase synchronization of two asymmetrically coupled smooth oscillators. (a) Reduced frequency vs reduced coupling strength. (b) Reduced frequency difference vs coupling strength showing frequency difference increase. $R = 10$–$1000\ \mathrm{k}\Omega$, $RC = 1$ s. (c) Current time series of oscillators before transition to synchronization. $R = 14\,706\ \Omega$, $C = 68\ \mu$F. (d) Current time series after transition to synchronization. $R = 10\,000\ \Omega$, $C = 100\ \mu$F. Dashed line, driver oscillator ($R_{\mathrm{ind},2} = 225\ \Omega$, $A_2 = 3.1\ \mathrm{mm}^2$); solid line, follower oscillator ($R_{\mathrm{ind},1} = 1000\ \Omega$, $A_1 = 0.8\ \mathrm{mm}^2$). $V = 1.090$ V.

The anomalous phase synchronization obtained with capacitive coupling can be compared to that obtained with resistive coupling at elevated temperature [32]. In a previous study the temperature was raised so that the oscillators had slightly elevated levels of nonisochronicity (for example, the average $qK_r = -0.35$). More importantly, the two oscillators exhibited different levels of nonisochronicity ($q_1K_r = -0.56$ vs $q_2K_r = -0.14$). Therefore, the advanced and delayed synchronization effects reported earlier are strongly affected by different levels of nonisochronicities (as predicted by theoretical and numerical studies [25]) and only a slight (7%) frequency difference enhancement was observed. In contrast, when the coupling is induced by capacitance, the nonisochronicity is approximately at the same level for each oscillator and the level is enhanced by about ten times compared to the resistive coupling. Because of the presence of strong nonisochronicity, a prominent frequency difference increase (about 50%) was observed during the transition synchronization and thus a robust anomalous phase synchronization effect was confirmed in the experimental system.

3. *Experiments with relaxation oscillators*

Experiments were also performed with relaxation oscillators that are obtained at higher potentials (e.g., $V = 1.315$ V). Previously it was found [36] that under these conditions the interaction function is deformed from the harmonic shape of the smooth oscillators and thus the synchronization transition occurred by a sequence of antiphase through complex to in-phase oscillations [16].

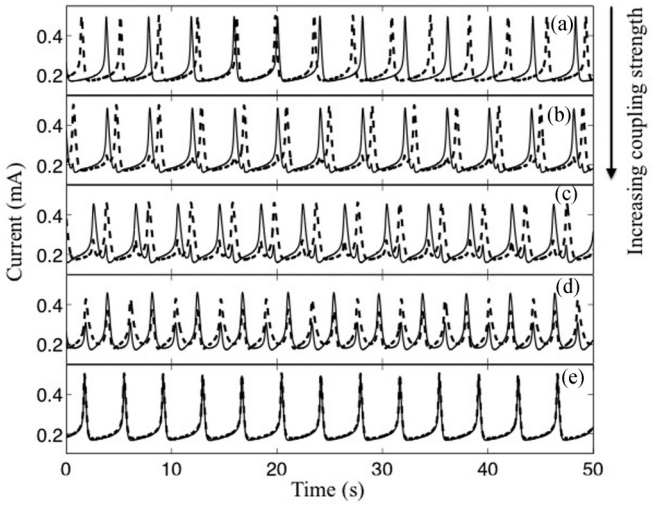

FIG. 6. Phase synchronization of two relaxation oscillators with capacitive coupling. Current time series of two relaxation oscillators. (a) No coupling. (b) Out-of-phase synchronization at $C = 50\ \mu$F. (c) Out-of-phase synchronization at $C = 150\ \mu$F. (d) Synchronization at $C = 500\ \mu$F with complex oscillatory wave form. (e) In-phase synchronization at $C = 1000\ \mu$F. $V = 1.315$ V, $R_{\mathrm{ind}} = 1200\ \Omega$.

Current time series of two relaxation oscillators with natural frequencies 0.248 and 0.275 Hz are shown in Fig. 6(a); note that in comparison with the smooth oscillators the periods of the relaxation oscillators are lengthened and the oscillatory wave form is now composed of alternations of a slow variation and a quick spike. The current time series of the oscillations with pure capacitive coupling ($C = 50\ \mu$F, 150 μF, 500 μF, and 1 mF) are shown in Figs. 6(b)–6(e), respectively. At a coupling strength comparable to that used with the smooth oscillators [$C = 50\ \mu$F, Fig. 6(b)], the oscillators synchronized in an out-of-phase configuration with a phase difference of 1.4 rad. This out-of-phase synchronization state is a robust response of the system; similar behavior was obtained with $C = 150\ \mu$F [Fig. 6(c)], where the phase difference is 2.0 rad. As the coupling was increased, the wave form of the oscillators developed small spikes at times when the other oscillators peaked; such small spikes that give period-2 character to the oscillations were also observed with resistive coupling, but in the negative direction [16]. With strong coupling at $C = 500\ \mu$F [Fig. 6(d)] the wave form is dramatically changed and exhibits a period-2 character due to the threshold response of the oscillators. If we consider the periodic cycle as the full period-2 wave form, the oscillators are antiphase synchronized. At very strong coupling strength, $C = 1$ mF [Fig. 6(e)], the oscillators are in-phase synchronized without any qualitative change of the oscillatory wave form.

In comparison with the synchronization of resistively coupled relaxation oscillators [16,36], several differences can be observed with the capacitive coupling. Relaxation oscillators required relatively strong resistive coupling (ten times stronger than smooth oscillators) to induce antiphase synchrony. With weak capacitive coupling the relaxation oscillations synchronize at about the same coupling strengths as the smooth oscillators and in out-of-phase configuration. At intermediate coupling strengths both coupling types induce

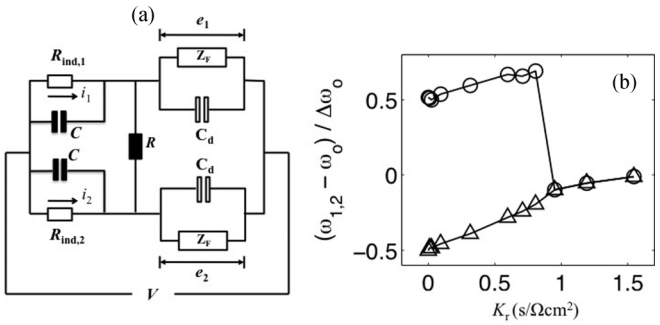

FIG. 7. Phase synchronization of two smooth oscillators with capacitance applied on individual resistances. (a) Equivalent circuit representation. (b) Reduced frequency difference vs reduced coupling strength graph showing positive nonisochronicity. $V = 1.180$ V, $R_{ind,1} = 1250\ \Omega$, $R_{ind,2} = 1000\ \Omega$, $R = 3$–$500\ \mathrm{k}\Omega$, $C = 1$ mF.

oscillations with complicated wave forms and structure; finally, at strong coupling both types of coupling result in identical synchronization of the oscillations.

B. Coupling with capacitance on individual resistors

Coupling of electrochemical oscillators with a capacitance could also be done by connecting the capacitors in parallel with the individual resistors as shown in the equivalent circuit of Fig. 7(a). In this configuration, the coupling interaction is purely through a resistance and thus not delayed, however, the electrochemical signal (current) is delayed through the use of the capacitance. We investigated the effect of capacitance on the governing equation of the electrochemical system and performed experiments with two symmetrically coupled oscillators to explore the extent of nonisochronicity in this configuration.

1. Theory

Kirchhoff's laws for the potentials and currents in this configuration obtained from Fig. 7(a) are as follows:

$$\begin{aligned} V &= e_1 + i_1 R_{\mathrm{ind},1}, \\ V &= e_2 + i_2 R_{\mathrm{ind},2}, \\ i_1 + C\frac{de_1}{dt} &= A_1 j_F(e_1) + A_1 C_d \frac{de_1}{dt} + \frac{e_2 - e_1}{R}, \\ i_2 + C\frac{de_1}{dt} &= A_2 j_F(e_2) + A_2 C_d \frac{de_2}{dt} + \frac{e_2 - e_1}{R}. \end{aligned}$$

The equations can be rearranged to give the dynamical equations for the electrode potentials as

$$\begin{aligned} \left(C_d + \frac{C}{A_1}\right)\frac{de_1}{dt} &= \frac{V - e_1}{A_1 R_{\mathrm{ind},1}} - j_F(e_1) + \frac{e_2 - e_1}{A_1 R}, \\ \left(C_d + \frac{C}{A_1}\right)\frac{de_2}{dt} &= \frac{V - e_2}{A_2 R_{\mathrm{ind},2}} - j_F(e_2) + \frac{e_1 - e_2}{A_2 R}. \end{aligned} \tag{13}$$

The equations thus indicate that by adding capacitance to the individual resistors the "effective" capacitance of the electrochemical oscillators can be tuned. The effect of capacitance on the synchronization properties is a complicated problem, since the phase interaction function (Γ) of the system could be altered because of the capacitance-induced change of the oscillator wave form and phase response curve.

2. Experiments with smooth oscillators

To explore the synchronization effect of an external capacitance applied on the individual resistors, we performed experiments with two smooth oscillators with $C = 1$ mF. The transition to phase synchronization is shown in Fig. 7(b). The reduced frequencies of both oscillators steadily increases with reduced coupling strength and phase synchronization occurs at $K_r^* = 0.95\ \mathrm{s}/\Omega\,\mathrm{cm}^2$. In contrast with the cross capacitance, the oscillators have positive nonisochronicity ($q_1 K_r{}^* = 0.33$ and $q_2 K_r{}^* = 0.37$) and the levels of nonisochronicity of the two oscillators are similar to each other. Thus we see that by applying capacitance on the individual resistors instead of the cross resistance, the sign of the nonisochronicity can be changed from negative to positive.

C. Comparison of coupling schemes

The different types of coupling schemes and their induced nonisochronicity levels for smooth oscillators obtained with nickel electrodissolution are summarized in Fig. 8. With difference (cross resistance) coupling [see Fig. 8(a)], at the commonly applied 283 K temperature, the oscillators are isochronous; therefore, it is not possible to observe anomalous phase synchronization effects with asymmetrical coupling. In a previous publication [32], we showed that with increase of temperature to 293 K, the two oscillators exhibited a weak, negative level of nonisochronicity (measured by q) [see Fig. 8(b)]. Because of the nonisochronicity, delayed and advanced phase synchronization were observed with asymmetrical coupling. However, because of the large

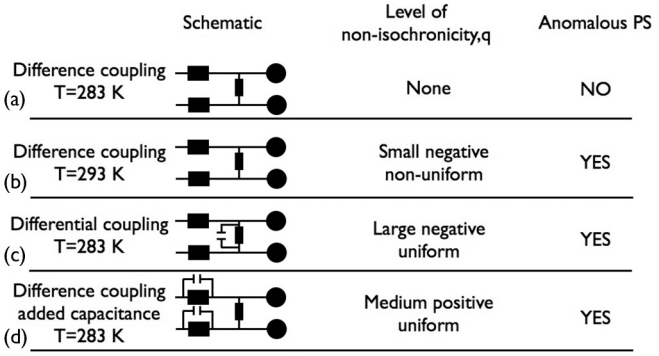

FIG. 8. Comparison of coupling schemes for oscillation isochronocity level and type, and the presence of anomalous phase synchronization effects with asymmetrical coupling (implemented using different electrode sizes) for smooth oscillators in Ni electrodissolution. (a) Difference coupling at 283 K with a cross resistance at low temperatures imposes no isochronocity. (b) Difference coupling at elevated temperature of 293 K imposes weak negative isochronicity; the level of isochronicity is greatly different for the two oscillators (nonuniform). (c) Differential coupling induces strong negative isochronicity which has approximately the same level for each oscillator (uniform). (d) Difference coupling with capacitance on individual resistors imposes moderate positive isochronicity. For each coupling scheme with induced isochronicities (b)—(d), anomalous phase synchronization effects [32] can be observed.

difference in the levels of nonisochronicity, the effect of another anomalous phase synchronization effect, frequency difference enhancement, was weak. As is demonstrated in this paper, differential coupling induces a strong, negative, uniform level of nonisochronicities and the expected strong frequency difference enhancement effect. Finally, when the capacitance is added to the individual resistors [with difference coupling; see Fig. 8(d)], the non-isochronicity is moderate and positive. The figure thus gives an overview of how several experimental conditions affect the level and uniformity of the nonisochronicity character of the oscillations.

IV. CONCLUSIONS

We showed that replacing the coupling resistance with capacitance has very strong impact on the observed synchronization dynamics of two electrochemical oscillators. The capacitance induces a differential coupling instead of the difference coupling of the resistance. Because of the fundamentally different coupling type, various synchronization patterns were found (e.g., coexistence of in- and antiphase synchrony with symmetrical coupling, frequency difference enhancement with asymmetrical coupling) that did not occur with resistive coupling under similar conditions. For relaxation oscillators weak coupling is an effective way of achieving out-of-phase synchronization. While cross capacitance induces negative nonisochronicity, capacitance on an individual resistance induces positive nonisochronicity in the interactions between the oscillators. The application of combined resistance and capacitance in the coupling process allows the effective tuning of the level of nonisochronicity (or "shear") of the oscillatory system. The overall level of nonisochronicity in the interaction between the oscillators plays an important role in the synchronization, especially in oscillator networks [28,46] and in the presence of asymmetrical coupling [25,30]. Recognition of the effect of the oscillator amplitude on the period has increasing relevance in analysis of biological (e.g., circadian) oscillators [47,48]; the experiments thus also provide examples of how the sensitive dependence of the period on the oscillator amplitude could affect synchronization patterns in pairs of symmetrically or asymmetrically coupled oscillators.

ACKNOWLEDGMENTS

This material is based upon work supported by the National Science Foundation under Grant No. CHE-0955555. Acknowledgement is made to the President's Research Fund of Saint Louis University for support of this research.

[1] M. Marek and I. Stuchl, Biophys. Chem. **3**, 241 (1975).
[2] H. Fujii and Y. Sawada, J. Chem. Phys. **69**, 3830 (1978).
[3] M. F. Crowley and I. R. Epstein, J. Phys. Chem. **93**, 2496 (1989).
[4] J. Miyazaki and S. Kinoshita, Phys. Rev. Lett. **96**, 194101 (2006).
[5] J. Weiner, R. Holz, F. W. Schneider, and K. Bar-Eli, J. Phys. Chem. **96**, 8915 (1992).
[6] M. J. B. Hauser and F. W. Schneider, J. Chem. Phys. **100**, 1058 (1994).
[7] D. Bilbao and J. Lauterbach, J. Catal. **272**, 309 (2010).
[8] M. Slinko, A. Ukharskii, and N. Jaeger, Phys. Chem. Chem. Phys. **3**, 1015 (2001).
[9] R. Imbihl, S. Ladas, and G. Ertl, Surf. Sci. **215**, L307 (1989).
[10] N. Nishiyama and K. Eto, J. Chem. Phys. **100**, 6977 (1994).
[11] R. Toth, A. F. Taylor, and M. R. Tinsley, J. Phys. Chem. B **110**, 10170 (2006).
[12] A. F. Taylor, M. R. Tinsley, F. Wang, Z. Huang, and K. Showalter, Science **323**, 614 (2009).
[13] M. Toiya, V. K. Vanag, and I. R. Epstein, Angew Chem. Int. Ed. **47**, 7753 (2008).
[14] M. Toiya, H. O. González-Ochoa, V. K. Vanag, S. Fraden, and I. R. Epstein, J. Phys. Chem. Lett. **1**, 1241 (2010).
[15] Z. Fei, R. Kelly, and J. L. Hudson, J. Phys. Chem. **100**, 18986 (1996).
[16] I. Z. Kiss, W. Wang, and J. L. Hudson, J. Phys. Chem. B **103**, 11433 (1999).
[17] A. Karantonis, M. Pagitsas, Y. Miyakita, and S. Nakabayashi, J. Phys. Chem. B **107**, 14622 (2003).
[18] J. M. Cruz, M. Rivera, and P. Parmananda, Phys. Rev. E **75**, 035201 (2007).
[19] Y. Mukouyama, H. Hommura, and T. Matsuda *et al.*, Chem. Lett. **25**, 463 (1996).
[20] K. Krischer, in *Modern Aspects of Electrochemistry*, edited by B. E. Conway, O. M. Bockris, and R. E. White (Kluwer Academic, New York, 1999), Vol. 32, p. 1.
[21] M. Wickramasinghe and I. Z. Kiss, in *Engineering of Chemical Complexity*, edited by G. Ertl and A. S. Mikhailov (World Scientific, Englewood Cliffs, NJ, 2013), p. 215.
[22] J. Christoph and M. Eiswirth, Chaos **12**, 215 (2002).
[23] Y. Kuramoto, *Chemical Oscillations, Waves and Turbulence* (Springer, Berlin, 1984).
[24] H. Sakaguchi and Y. Kuramoto, Prog. Theor. Phys. **76**, 576 (1986).
[25] B. Blasius, Phys. Rev. E **72**, 066216 (2005).
[26] E. Montbrio and B. Blasius, Chaos **13**, 291 (2003).
[27] B. Blasius, E. Montbrio, and J. Kurths, Phys. Rev. E **67**, 035204 (2003).
[28] H. Daido and K. Nakanishi, Phys. Rev. Lett. **96**, 054101 (2006).
[29] E. Montbrio and D. Pazó, Phys. Rev. Lett. **106**, 254101 (2011).
[30] S. K. Dana, B. Blasius, and J. Kurths, Chaos **16**, 023111 (2006).
[31] I. T. Tokuda, S. K. Dana, and J. Kurths, Chaos **18**, 023134 (2008).
[32] M. Wickramasinghe, E. M. Mrugacz, and I. Z. Kiss, Phys. Chem. Chem. Phys. **13**, 15483 (2011).
[33] U. F. Franck and L. Meunier, Z. Naturforschg. **8b**, 396 (1953).
[34] A. J. Bard and L. R. Faulkner, *Electrochemical Methods* (Wiley, New York, 2000).
[35] O. Lev, A. Wolffberg, L. M. Pismen, and M. Sheintuch, J. Phys. Chem. **93**, 1661 (1989).
[36] I. Z. Kiss, Y. M. Zhai, and J. L. Hudson, Phys. Rev. Lett. **94**, 248301 (2005).

[37] A. S. Pikovsky, M. G. Rosenblum, G. V. Osipov, and J. Kurths, Physica D **104**, 219 (1997).
[38] I. Z. Kiss, Q. Lv, and J. L. Hudson, Phys. Rev. E **71**, 035201 (2005).
[39] S. H. Strogatz, Physica D **143**, 1 (2000).
[40] J. Miyazaki and S. Kinoshita, Phys. Rev. E **74**, 056209 (2006).
[41] C. G. Rusin, I. Tokuda, I. Z. Kiss, and J. L. Hudson, Angew. Chem. Int. Ed. **50**, 10212 (2011).
[42] H. Kori, C. G. Rusin, I. Z. Kiss, and J. L. Hudson, Chaos **18**, 026111 (2008).
[43] C. G. Rusin, H. Kori, I. Z. Kiss, and J. L. Hudson, Philos. Trans. R. Soc., A **368**, 2189 (2010).
[44] A. S. Pikovsky, M. G. Rosenblum, and J. Kurths, *Synchronization- A Universal Concept in Nonlinear Sciences* (Cambridge University Press, Cambridge, England, 2001).
[45] I. Z. Kiss, C. G. Rusin, H. Kori, and J. L. Hudson, Science **316**, 1886 (2007).
[46] D. M. Abrams and S. H. Strogatz, Phys. Rev. Lett. **93**, 174102 (2004).
[47] U. Abraham, A. E. Granada, P. O. Westermark, M. Heine, A. Kramer, and H. Herzel, Mol. Syst. Biol. **6**, 438 (2010).
[48] S. Schroder, E. D. Herzog, and I. Z. Kiss, J. Biol. Rhythms **27**, 79 (2012).